Variable-range hopping conductivity and absence of a true metal–insulator transition in $La_{0.7-\delta}Ca_{0.3}Mn_{1-y}Fe_yO_3$

R. Laiho, E. Lähderanta, and J. Salminen
Wihuri Physical Laboratory, University of Turku, FIN-10014 Turku, Finland

K. G. Lisunov and V. S. Zakhvalinskii
Institute of Applied Physics, Academiei Str., 5, MD-2028 Kishinev, Moldova

M. O. Safontchik, M. A. Shakhov, and M. L. Shubnikov
A. F. Ioffe Physico-Technical Institute, 194021 St. Petersburg, Russia

Resistivity of $La_{0.7-\delta}Ca_{0.3}Mn_{1-y}Fe_yO_3$ (LCMFO) with $y=0-0.05$, $\delta=0$ and 0.017 is investigated between 4.2–350 K, showing that La vacancies increase the effect of Fe doping by influencing electronic states through additional microscope disorder. The Shklovskii–Efros variable-range hopping conductivity, governed by generation of a soft parabolic gap in the spectrum of localized states due to Coulomb interaction between charge carriers, is observed both above and well below the ferromagnetic-to-paramagnetic transition temperature. Our results give evidence for absence of a true metal–insulator transition both in undoped material and in LCMFO. © *2002 American Institute of Physics.* [DOI: 10.1063/1.1448300]

The mixed-valence manganite perovskite $La_{1-x}Ca_xMnO_3$, briefly LCMO, containing Mn^{3+} and Mn^{4+} shows the ''colossal'' magnetoresistance (CMR) near the paramagnetic (PM) to ferromagnetic (FM) transition temperature, T_C.[1] Attention has been paid also to $La_{1-x}Ca_xMn_{1-y}Fe_yO_3$ (LCMFO) where due to similar ionic radii of Mn^{3+} and Fe^{3+} only minor lattice distortions are expected by the substitution.[2] At a low doping level, $y=0.01-0.05$, Fe^{3+} ions diminish slightly the concentration of Mn^{4+}, i.e., c, and introduce additional antiferromagnetic interactions in the system.[3] However, the strong influence on transport and magnetic properties[2,4] is incompatible with the small decrease of c. This suggests a substantial increase of interatomic disorder by Fe doping. To verify this conjecture we have introduced additional disorder to LCMFO by creation of a small amount of La vacancies (for $c\approx x\approx 0.3$ the concentration of vacancies $\delta\sim 0.01$ increases c by $3\delta\sim 0.03 \ll c$).

Samples of $La_{1-x-\delta}Ca_xMn_{1-y}Fe_yO_3$ with $x=0.3$, $y=\delta=0$ (sample # 3-0) and $x=0.3$, $\delta\approx 0.017$, $y=0.01$ (sample # 3-1) and $y=0.05$ (sample # 3-5) were synthesized with standard ceramic procedure, having the same cubic structure as the undoped material.[5]

The dependencies of $\chi(T)=M_{dc}(T)/B$, measured in the field of 2 G in zero-field cooled (ZFC), field-cooled (FC) and in the thermoremanent magnetization (TRM) regime, are basically similar to those shown in Fig. 1 for # 3-1, with $T_C=259$ K, 236 K, and 164 K for # 3-0, 3-1, and 3-5, respectively. Deviation of $\chi_{ZFC}(T)$ from $\chi_{FC}(T)$ reflects frustration of the magnetic state below T_C as in LCMO.[5] The sharp peak of $\chi_{FC}(T)$ just below T_C is attributed to the onset of charge ordering.[6]

As evident from Fig. 1 $\rho(T)$ has at $T_m\approx T_C$ a maximum and increases drastically for # 3-1 and # 3-5 with respect to # 3-0. At the same time T_m is shifted to a lower temperature. In comparison with the existing data for $\delta=0$ and similar x,[2,4,7] in our LCMFO samples the shift of T_m with y is larger and the ratio $\rho(T_m,y)/\rho(T_m,0)$ is increased by 2–3 orders of magnitude. Hence, creation of La vacancies increases the effects of doping with Fe.

Below we distinguish between two types of disorder in CMR materials. The mechanism proposed by Varma[8] treats the PM–FM transition in La manganites by considering the localization of charge carriers, due to slow fluctuations of spin configuration and Coulomb interactions, inside a band of width W. According to this model $kT_C\approx 0.05\ Wc(1-c)$. The disorder introduced by Fe favors the localization of the carriers by decreasing the localization radius a, resulting in narrowing of W and, consequently, in decrease of T_C when y is increased. Taking $c\approx 0.3(\delta=0)$ and ≈ 0.35 ($\delta=0.017$), we obtain $W\approx 2.1$ eV, 1.8 eV, and 1.2 eV for # 3-0, 3-1, and 3-5, respectively. Another type of disorder con-

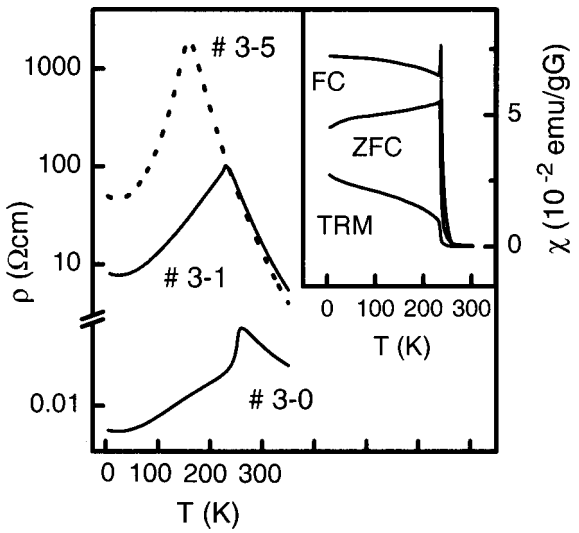

FIG. 1. Results of $\rho(T)$ for # 3-0, 3-1, and 3-5 and $\chi(T)$ for # 3-1 (inset).

nected not to a but to random energy barriers generated by the noncollinearity of the spin system, was proposed by Viret *et al.*[9] In zero field it becomes important below T_C due to appearance of local magnetization, M, which reduces the average height of the random barriers and decreases W.[9]

It is generally believed that in CMR materials $\rho(T)$ is governed above T_C by hopping of small polarons connected to local Jahn–Teller distortions, and that the large drop of $\rho(T)$ close to T_C at $x \approx 0.33$ is due to the metal–insulator transition.[10] When hopping of charge carriers beyond the nearest sites is energetically favorable, the variable-range hopping (VRH) conductivity sets in,[11] leading to the resistivity

$$\rho(T) = \rho_0(T) \exp[(T_0/T)^p], \tag{1}$$

with $T_0 = Qa^{1-1/p}$. When the Coulomb interaction between the hopping carriers is unimportant, we have $p = 1/4$ and $Q = \alpha/[kg(\mu)]$, where $\alpha = 18$, $g(E)$ is the density of localized states (DOS) at the energy E, and μ is Fermi level (the Mott–VRH).[11] In the opposite case the Coulomb interaction creates a soft parabolic gap with width Δ in the DOS around μ, that gives $p = 1/2$ [the Shklovskii–Efros (SE) VRH].[12] If $\Delta < W$, we have $Q = \beta_1 e^2/(k\kappa)$, $\Delta = 2e^3 g_0^{1/2}/\kappa^{1/212}$ and the value of DOS outside the gap is $g_0 = N_0/(W - 2\Delta/3)$, where $\beta_1 = 2.8$,[12] κ is the dielectric permeability and N_0 is the concentration of the localized states. In the case of $\Delta > W$, means that $g(E) \sim (E-\mu)^2$ inside the whole band, we obtain $Q = \beta_2 W/(N_0^{1/3} k)$, where $\beta_2 = 1.2$.

For $\Gamma \equiv [kT(T_0/T)^p a/(2\hbar s)]^2 \ll 1$ (s is the sound velocity), the dependence of ρ_0 on T is weak and can be neglected.[12] For $\Gamma \gg 1$ we find $\rho_0(T) = AT^m$, where $A = (C/2^q) a^{11} T_0^{(7+q)p}$, $C = 9\pi\sigma d \kappa^2 k^8/(256 E_1^2 e^6 s^3 \hbar^4)$, $\sigma = 2p(1-p)$, d is the material density and E_1 is the deformation potential constant. For a conventional wave function of localized carriers, $\Psi(r) \sim \exp(-r/a)$, we have $q = 0$ and $m = 25/4$ and $9/2$ for $p = 1/4$ and $p = 1/2$, respectively. However, the microscopic structural defects introduce an additional short-range potential, changing $\Psi(r)$ to $\Psi(r) \sim r^{-1} \exp(-r/a)$[12] that gives $q = 4$ and $m = 21/4$ and $5/2$ for $p = 1/4$ and $p = 1/2$, respectively.

Assuming constant ρ_0, we obtain above T_C the values of Γ between 20–80 ($s = 6.8 \times 10^5$ cm/s for LCMO[13]). Then the dependence of ρ_0 on T cannot be neglected for both VRH regimes. To determine p and m in this situation, we present the local activation energy.[12] $E_a(T) \equiv d \ln \rho(T)/d(kT)^{-1}$, in the form $\ln[E_a(T)/(kT)+m] = \ln p + p \ln T_0 + p \ln(1/T)$. In this equation m is varied and the functions $p(m)$ are determined from the slopes of the plots $\ln[E_a(T)/(kT)+m]$ vs $\ln(1//T)$. As shown in Fig. 2, the plot $p(m)$ for each sample gives a single pair of (p,m) for different types of $\Psi(r)$ and VRH regime. For all samples the value of $p \approx 0.5$, corresponding to the SE–VRH, is found, while $m \approx 4.5$ for # 3-0 is changed to $m \approx 2.5$ for # 3-1 and 3-5. This gives evidence that doping with Fe influences the electronic properties of LCMO by inducing microscopic structural disorder.

Above T_m the plots of $\ln[\rho/T^m]$ vs $T^{-1/2}$ shown in Fig. 3 are linear functions giving $A = 2.7 \times 10^{-20}$ Ω cm K$^{-9.2}$, 2.8×10^{-14} Ω cm K$^{-5/2}$, and 5.3×10^{-15} Ω cm K$^{-5/2}$ and $T_0 = 8.1 \times 10^4$ K, 1.2×10^5 K, and 1.3×10^5 K for # 3-0, 3-1, and 3-5, respectively. The values of $\Delta = 0.44$ eV, 0.54 eV, and 0.59 eV for # 3-0, 3-1, and 3-5, respectively, are obtained with equation $\Delta \approx k(T_0 T_v)^{1/2}$,[12] where $T_v = 319$, 344, and ≈ 350 K is the temperature of the onset of the SE–VRH regime. Using the values of T_0, A, Δ, $W > \Delta$, and $N_0 = 1.74 \times 10^{22}$ cm^{-3}, we evaluate with the equations $\kappa = 2^{2/3} e^2 g_0^{1/3}/\Delta^{2/3}$, $a = [2^m/(Ck^q)]^{1/11} T_0^{-(7+q)/22} A^{1/11}$, and $\beta_{1ex} = T_0 \kappa k a/e^2$: $\kappa = 8.4$, 7.9, and 8.9, $a = 6.1$ Å, 3.0 Å, and 2.3 Å, and $\beta_{1ex}/\beta_1 = 9.1$, 5.9, and 6.0, where β_{1ex} is the value of β_1 obtained experimentally. In these calculations we

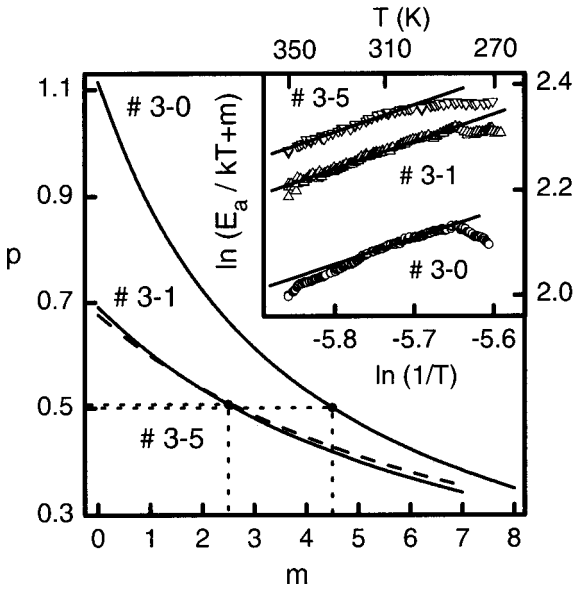

FIG. 2. Dependence of p on m. Inset: $\ln(E_a/kT+m)$ vs $\ln(1/T)$ for $m = 9/2$ (# 3-0) and 5/2 (# 3-1 and 3-5).

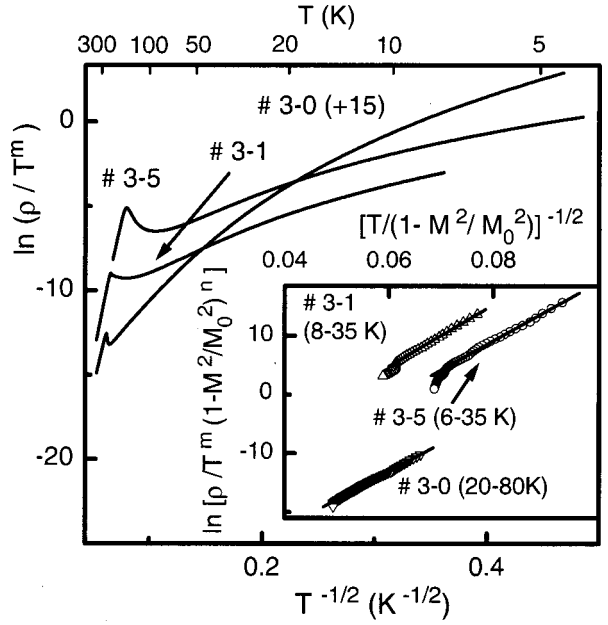

FIG. 3. Dependence of $\ln(\rho/T^m)$ on $T^{-1/2}$ for # 3-0 ($m = 9/2$, shifted by +15 units along Y axis), # 3-1 and # 3-5 ($m = 5/2$). Inset: $\ln[\rho/T^m(1-M^2/M_0^2)^n]$ vs $[T/(1-M^2/M_0^2)]^{-1/2}$ for # 3-0 ($m = 9/2$ and $n = 7/2$), # 3-1 and # 3-5 ($m = 5/2$ and $n = 11/2$). In brackets are the temperature intervals for linear dependence.

use $E_1 \approx GW(dT_C/dp)/(6T_C) \approx 5.8$ eV, estimated from the baricity coefficient $(dT_C/dp) \approx 0.9$ K/kbar at $T_C = 271$ K for LCMO with $x = 0.33$[14] and the Young modulus $G \approx 5 \times 10^{11}$ N/m^2.[15]

As evident from Fig. 3, the interval of metallic-like behavior (decrease of $\ln[\rho/T^m]$ vs $T^{-1/2}$) is observed only within a narrow interval below T_m, while with further lowering of T the activated character of ρ is restored. However, the plots of $\ln[\rho/T^m]$ vs $T^{-1/2}$ are nonlinear functions in this temperature interval. This can be connected to change of the dominating disorder from the Varma type[8] at $T > T_C$ to that predicted by Viret *et al.*[9], at $T < T_C$. For the latter $W(T) = U_m[1 - M^2(T)/M_0^2]$ decreases with T, where $U_m \approx 2$ eV,[9] and for $W < \Delta T_0$ depends on T according to $T_0(T) = T_0^*[1 - M(T)^2/M_0^2]$, where $T_0^* = \beta_2 U_m/(N_0^{1/3} ka)$. As shown in the inset to Fig. 3, the plots of $\ln[\rho/T^m(1-M^2/M_0^2)^n]$ vs $[T/(1-M^2/M_0^2]^{-1/2}$ (here $n = 7/2$ for # 3-0 and 11/2 for # 3-1 and 3-5) can be represented by linear functions below T_m, where the local magnetization is taken to be equal to TRM (inset to Fig. 1), and M_0 is found by extrapolation of the plots of TRM to $T = 0$. In a way similar to the case of $T > T_m$ and $W > \Delta$ and utilizing the values of κ obtained above, we find $T_0^* = 2.3 \times 10^5$ K, 2.7×10^5 K, and 2.4×10^5 K, $a = 5.9$ Å, 3.0 Å, and 2.3 Å and $\beta_{2ex}/\beta_2 = 8.6$, 7.3, and 4.9.

Hence, doping with Fe decreases a, which agrees with influence of Fe on electronic properties of LCMO by increasing the atomic-scale disorder. The values of β_1 and β_2 are enhanced with respect to those predicted in the SE model for doped semiconductors, which may be connected with the polaronic character of charge carriers in LCMO and LCMFO. We find $\beta_{1ex}/\beta_1 \approx \beta_{2ex}/\beta_2$ and essentially the same values of a for $T > T_m$ and at $T < T_m$.

Because the VRH conductivity is observed on both sides of $T_m \approx T_C$ and at $T \ll T_m$, a true metal–insulator transition exists neither in LCFMO, nor in LCMO. The alternation of the hopping and metallic conductivity found above can be explained by an interplay between the phase separation and the charge ordering effects, both being intrinsic properties of CMR compounds. As $T \to T_C$, the FM metallic phase, constituting of small separated particles[16,17] in the semiconducting PM host well above T_C, increases forming percolation clusters. Therefore, the onset of the metallic behavior near T_C corresponds to the percolation threshold or generation of an infinite cluster. Below T_C this cluster is destroyed by the onset of charge ordering and the hopping conductivity pertinent to the host phase is restored.

[1] P. Schiffer, A. P. Ramirez, W. Bao, and S.-W. Cheong, Phys. Rev. Lett. **75**, 3336 (1995).
[2] K. H. Ahn, X. W. Wu, K. Liu, and C. L. Chien, Phys. Rev. B **54**, 15 299 (1996).
[3] A. Simopoulos, M. Pissas, G. Kallias, E. Devlin, N. Moutis, I. Panagiotopoulos, D. Niarchos, C. Christides, and R. Sonntag, Phys. Rev. B **59**, 1263 (1999).
[4] S. K. Hasanain, M. Nadeem, W. H. Shah, M. J. Akhtar, and M. M. Hasan, J. Phys.: Condens. Matter **12**, 9007 (2000).
[5] R. Laiho, K. G. Lisunov, E. Lähderanta, P. A. Petrenko, V. N. Stamov, and V. S. Zakhvalinskii, J. Magn. Magn. Mater. **213**, 271 (2000).
[6] Y. Moritomo, Phys. Rev. B **60**, 10 374 (1999).
[7] K. Ghosh, S. B. Ogale, R. Ramesh, R. L. Greene, T. Venkatesan, K. M. Gapchup, R. Bathe, and S. I. Patil, Phys. Rev. B **59**, 533 (1999).
[8] C. M. Varma, Phys. Rev. B **54**, 7328 (1996).
[9] M. Viret, L. Ranno, and J. M. D. Coey, Phys. Rev. B **55**, 8067 (1997).
[10] A. P. Ramirez, J. Phys.: Condens. Matter **9**, 8171 (1997).
[11] N. F. Mott, *Metal-Insulator Transitions* (Taylor & Francis, London, 1990).
[12] B. I. Shklovskii and A. L. Efros, *Electronic Properties of Doped Semiconductors* (Springer, Berlin, 1984).
[13] R. K. Zheng, C. F. Zhu, J. Q. Xie, and X. G. Li, Phys. Rev. B **63**, 024427 (2000).
[14] V. Laukh, J. Fontcuberta, J. L. Garcia-Munoz, and X. Obradors, Phys. Rev. B **56**, R10009 (1997).
[15] V. Moshnyaga, S. Klimm, E. Gommert, R. Tidecks, S. Hom, and K. Samwer, J. Appl. Phys. **88**, 5305 (2000).
[16] M. Hennion, F. Moussa, G. Biotteau, J. Rodriguez-Carvajal, L. Piusard, and A. Revcolevschi, Phys. Rev. Lett. **81**, 1957 (1998).
[17] V. Chechersky, A. Nath, I. Isaac, J. P. Franck, K. Ghosh, H. Ju, and R. L. Greene, Phys. Rev. B **59**, 497 (1999).